

Local Mirror Symmetry at Higher Genus

Albrecht Klemm* and Eric Zaslow**

**School of Natural Sciences, IAS, Olden Lane, Princeton, NJ 08540, USA*

***Department of Mathematics, Northwestern University, Evanston, IL 60208, USA*

Abstract

We discuss local mirror symmetry for higher-genus curves. Specifically, we consider the topological string partition function of higher-genus curves contained in a Fano surface within a Calabi-Yau. Our main example is the local \mathbf{P}^2 case. The Kodaira-Spencer theory of gravity, tailored to this local geometry, can be solved to compute this partition function. Then, using the results of Gopakumar and Vafa [1] and the local mirror map [2], the partition function can be rewritten in terms of expansion coefficients, which are found to be integers. We verify, through localization calculations in the A-model, many of these Gromov-Witten predictions. The integrality is a mystery, mathematically speaking. The asymptotic growth (with degree) of the invariants is analyzed. Some suggestions are made towards an enumerative interpretation, following the BPS-state description of Gopakumar and Vafa.

* e-mail: klemm@ias.edu

** e-mail: zaslow@math.nwu.edu

1. Introduction and Summary

In [2], the techniques of mirror symmetry were applied to the local geometry of a Fano surface inside a Calabi-Yau manifold. Namely, from the data of the canonical bundle of the surface, differential equations were proposed whose solutions yield genus-zero, Gromov-Witten-type invariants.¹ From these, one arrives at integers after accounting for contributions from multiple coverings. The mirror symmetry predictions were corroborated by independent A-model calculations using localization. The mirror principle was the main tool used for verification; some more explicit fixed point calculations were made, as well. Excess intersection considerations showed that the integers represent the *effective number* of rational curves “coming from” the Fano surface.

In this paper, we extend these techniques to higher-genus curves. For the A-model calculations, we use localization techniques on higher-genus moduli spaces to compute the Gromov-Witten invariants. The mirror principle does not apply at higher genus. The analogue of the prepotential at higher genus is the topological partition function at genus g , whose coefficients are the Gromov-Witten invariants.

For the B-model, equations governing the dependence of these partition functions, $F^{(g)}$, on the complex structure moduli of the Calabi-Yau were found in [3][4]. In the effective 4-d N=2 supergravity theory, emerging from type IIB string theory compactification on the Calabi-Yau, the $F^{(g \geq 1)}$ appear as coefficients of the $\mathcal{R}^2 \mathcal{F}^{2g-2}$ terms (here \mathcal{R} and \mathcal{F} are the self-dual parts of the Riemann tensor and the graviphoton field strength, respectively).² The recursive nature of the equations comes from the fact that Riemann surfaces with marked points degenerate at the boundaries of moduli space – either into pairs of lower-genus surfaces or surfaces with fewer marked points. As the anti-holomorphic dependence of the topological partition functions is determined by an exact form, it only receives contributions from the boundaries.

One can tailor the methods of [4] to the local situation we seek. Our motivation for doing so depends on two simplifications in the local case. First, the solution of the holomorphic anomaly equation using Kodaira-Spencer gravity simplifies considerably in

¹ These invariants are like the relative invariants of Ionel and Parker, except that the degenerations are sort of “one-sided.”

² The genus zero prepotential $F^{(0)}$ determines the gauge kinetic terms and the masses of the charged BPS states. The information contained in the local geometry suffices to obtain the rigid theory (Seiberg-Witten theory) – see [5] for reviews.

the local case due to the fact that the propagators involving the descendents of the puncture operator (2-d dilaton) can be gauged to zero. Second, the higher-genus Gromov-Witten invariants are computable using localization. This is in contrast to complete-intersection Calabi-Yau manifolds in toric varieties, where the moduli space of higher-genus maps into the Calabi-Yau is not simply expressible as the zero locus of a section of a bundle over the moduli space of maps into an ambient toric manifold.³ For Fano surfaces which are themselves toric, we need not cut with a section to obtain the moduli space of interest. This implies in particular that calculations can be made to fix the ambiguity in solving the Kodaira-Spencer recursions in the local case. In the global case of the quintic, by contrast, classical geometry cannot fix certain unknown constants.

After solving the Kodaira-Spencer theory and using the mirror map, we verify mirror symmetry and apply the work of Gopakumar and Vafa [1] to organize the topological partition functions in terms of coefficients which should be integers, as they count BPS states of specified spin and charge (in the four-dimensional theory, spin refers to a Lefschetz-type $SU(2)$ action on the BPS states). This integrality check is a strong test of the power of M-theory and the approach of Gopakumar and Vafa. The asymptotic growth of the invariants is also analyzed directly.

The mathematical interpretation of these integers is still unclear. A proper explanation seems to involve moduli spaces of objects in derived categories. Heuristic evidence exists in support of this observation.

Another explanation is lacking. The form of the partition functions predicted by Gopakumar and Vafa is a generalization of the multiple cover formula ($1/k^3$). The multiple cover formula is well-understood mathematically, but the higher-genus generalizations are a mystery.

We would like to note that Hosono, Saito, and Takahashi [6] obtain BPS counts and compute topological partition functions via B-model calculations for the rational elliptic surface, though their techniques are somewhat different. They achieve good corroboration of Vafa and Gopakumar's formulas. A-model calculations for this surface would presumably be prohibitive. Moore and Marino also have achieved higher-genus results via heterotic duality [7].

³ We thank R. Pandharipande for explaining this to us.

2. Localization at Higher Genus

The tools for the localization calculations have been available since the work of Kontsevich [8], Li-Tian [9], Behrend-Fantechi [10], Graber-Pandharipande [11], and Faber [12].

The moduli space, $\overline{\mathcal{M}}_{g,0}(\beta; \mathbf{P})$, of stable maps from genus g curves into some toric variety \mathbf{P} with image in $\beta \in H_2(\mathbf{P}; \mathbf{Z})$ can have components of various dimensions. To do intersection theory on it, we need a fundamental cycle of some “appropriate” dimension – the virtual fundamental class.

This procedure was developed in [10], and the equivariant localization for spaces with perfect deformation theories was developed in [11]. In that paper, the authors treat the case of interest to us: the restrictions to the fixed point loci (under the torus action) of the equivariant fundamental cycle on the space of holomorphic maps of genus g . The authors give explicit formulas for the weights.

In our examples, we are interested in calculating Chern classes of U_β , the bundle over moduli space whose fiber at a point $(C, f) \in \overline{\mathcal{M}}_{g,0}(\beta; \mathbf{P})$ is equal to $H^1(C, f^*K_{\mathbf{P}})$. It is not difficult to compute the equivariant Chern classes at the fixed loci.

Using these ingredients, we can perform localization calculations at higher genus. The Atiyah-Bott fixed point formula – true for virtual classes by [11] – reduces the calculation to integrals over these fixed loci. The different components of the fixed loci are represented by different graphs. We sum over the graphs using a computer algorithm. As all the higher-genus behavior must be centered at the fixed points (there are no fixed higher-genus curves), the fixed loci are all products of moduli spaces of curves, and the graphs are decorated by genus data at each vertex as well as degree data at each edge, as in [8]. The integrals over the moduli spaces are performed using the algorithm of Faber [12].

In the following subsections, we summarize this procedure.

2.1. Localization Formulas

As discussed in [2], a Fano surface within a complete-intersection Calabi-Yau contributes to the Gromov-Witten invariants, producing an effective “number” of rational curves. In fact, the curves are not isolated and there is a whole moduli space of maps into the Fano surface, arising as a non-discrete zero locus of a section of a bundle over the moduli space of maps in the Calabi-Yau. Just as spaces of multiple coverings of isolated

curves contribute to the Gromov-Witten invariants by the excess intersection formula,⁴ the contribution from the surface B can be calculated as well. It is

$$K_\beta^g = \int_{\overline{\mathcal{M}}_{g,0}(\beta;B)} c(U_\beta), \quad (2.1)$$

where $\beta \in H_2(B; \mathbf{Z})$ and U_β is the bundle whose fiber over $(C, f) \in \overline{\mathcal{M}}_{g,0}(\beta; B)$ is the vector space $H^1(C, f^*K_B)$.⁵

We assume that B has a toric description so that we may use the torus action to define an action on $\overline{\mathcal{M}}_{0,0}(\beta; B)$ (moving the image curves) and on U_β , which inherits the natural action on the canonical bundle. We evaluate the Gromov-Witten invariants by localizing to the fixed points using the Atiyah-Bott formula

$$\int_M \phi = \sum_P \int_P \left(\frac{i_P^* \phi}{e(\nu_P)} \right),$$

where the sum is over fixed point sets P , i_P is the embedding into M , and $e(N_{P/M})$ is the Euler class of the normal bundle of P in M .

Graber and Pandharipande proved that this formula holds *mutatis mutandis*, with the replacement of the integral of a class by evaluation over virtual fundamental cycles (in the equivariant Chow ring) of equivariant classes of deformation complexes. The equivariant Chern classes and bundles involved are then computed in the standard way, e.g. by looking at the weights of sections and taking alternating products over terms in a complex. In our case, following Kontsevich, the fixed moduli can be labeled by graphs. The fixed locus $\overline{\mathcal{M}}_\Gamma$ corresponding a graph Γ is a product of moduli spaces:

$$\overline{\mathcal{M}}_\Gamma = \prod_v \overline{\mathcal{M}}_{g(v), val(v)}.$$

Here v are the vertices of the graph and $g(v)$ and $val(v)$ are the genus and valence of the vertex. (At a vertex, which is mapped to a torus fixed point, the choice of a $val(v)$ -marked genus $g(v)$ curve represents the only moduli.)

⁴ The contribution, from a component of the zero locus Y of some section, to the Chern class $c(E)$ of some vector bundle E over M is $\int_Y \frac{c(E)}{c(N_{Y/M})}$, where $N_{Y/M}$ represents the normal bundle of Y in M . The equation here follows from the reasoning between eqs. (5.4) and (5.5) in [2].

⁵ Let ev be the evaluation map from $\overline{\mathcal{M}}_{g,1}(\beta; B)$ to B and let π be the map $\overline{\mathcal{M}}_{g,1}(\beta; B) \rightarrow \overline{\mathcal{M}}_{g,0}(\beta; B)$ which forgets the marked point. Then $U_\beta = \mathcal{R}^1 \pi_* ev^* K_B$.

Graber and Pandharipande [11] found the weights of the inverse of the Euler class of the normal bundle to be:

$$\begin{aligned}
\frac{1}{e(N^{vir})} &= \prod_e \frac{(-1)^{d_e} d_e^{2d_e}}{(d_e!)^2 (\lambda_{i(e)} - \lambda_{j(e)})^{2d_e}} \prod_{\substack{a+b=d_e \\ a,b \geq 0 \\ k \neq i(e), j(e)}} \frac{1}{\frac{a}{d_e} \lambda_{i(e)} + \frac{b}{d_e} \lambda_{j(e)} - \lambda_k} \\
&\times \prod_v \prod_{j \neq i(v)} (\lambda_{i(v)} - \lambda_j)^{val(v)-1} \\
&\times \begin{cases} \prod_v \left[\left(\sum_F w_F^{-1} \right)^{val(v)-3} \prod_{F \ni v} w_F^{-1} \right] & \text{if } g(v) = 0 \\ \prod_v \prod_{j \neq i(v)} P_{g(v)}(\lambda_{i(v)} - \lambda_j, E^*) \prod_{F \ni v} \frac{1}{w_F - e_F} & \text{if } g(v) \geq 1 \end{cases} \quad (2.2)
\end{aligned}$$

where the case with $g(v) = 0$ is from [13]. Here $i(v)$ is the fixed-point image of the vertex v ; edges e represent invariant \mathbf{P}^1 's connecting the fixed point labeled $i(e)$ to $j(e)$; and flags F are pairs (v, e) of vertices and edges attached to them. $\omega_F = (\lambda_{i(F)} - \lambda_{j(F)})/d_e$, where $i(F) = i(e)$ and $j(F) = j(e)$ for the associated edge $e \in F$. e_F is the Chern class of the line bundle over M_Γ whose fiber is the point $e(F) \cap C_v$, a “gravitational descendant” in physical terms – also known as a κ class. We have defined the polynomial $P_g(\lambda, E^*) = \sum_{r=0}^g \lambda^r c_{g-r}(E^*)$, where E is the Hodge bundle with fibers $H^0(K_C)$ on moduli space.

The bundle U_β , whose top Chern class ϕ we are calculating, has fibers $H^1(C, f^*K_B)$ over a point (C, f) . Let us now fix $B = \mathbf{P}^2$ and put $\beta = d$ since $H_2(\mathbf{P}^2)$ is one-dimensional. Since the invariant maps are known and the maps from the genus $g(v) > 0$ pieces are constants, we explicitly calculate the weights of the numerator in the Atiyah-Bott formula to be:

$$i^*(\phi) = \prod_v \Lambda_{i(v)}^{val(v)-1} P_{g(v)}(\Lambda_{i(v)}, E^*) \prod_e \left[\prod_{m=1}^{3d_e-1} \Lambda_{i(e)} + \frac{m}{d_e} (\lambda_{i(e)} - \lambda_{j(e)}) \right], \quad (2.3)$$

where $\Lambda_i = \lambda_1 + \lambda_2 + \lambda_3 - 3\lambda_i$.

2.2. Faber's algorithm

We therefore have explicit formulas for the class to integrate along \overline{M}_Γ . The integrals involve the κ classes and the Mumford classes (from the Hodge bundle). The integrals can be performed by the recursive algorithm developed by Faber.

A rough sketch of the idea of Faber's algorithm is as follows [12]. Witten's original recursion relations from topological gravity [14], proved by Kontsevich [15], suffice to determine integrals of powers of the ψ_i 's, which are the first Chern classes of the line bundles whose fiber is the cotangent space of the corresponding marked point, $i = 1, \dots, n$ (the gravitational descendents). However, the integrals over $\overline{\mathcal{M}}_\Gamma$ involve the λ classes as well – the Chern classes of the Hodge bundle. These classes can be represented by cycles involving the boundary components of moduli space as well as the ψ_i 's.

So a proper intersection theory including boundary classes is needed. The boundary components are images under maps from $\overline{\mathcal{M}}_{g-1, n+2}$ (the map identifying the last two points; this map is of degree two since swapping the points gives the same boundary curve) and $\overline{\mathcal{M}}_{h, s+1} \times \overline{\mathcal{M}}_{g-h, (n-s)+1}$ (the map identifying the two last points, which is degree one except when both $n = 0$ and $h = g/2$). Understanding the pull-back of the boundary classes under these maps completes the reduction of intersection calculations to lower genera. For example, the ψ_i 's pull back to ψ_i 's of corresponding points in the new moduli spaces. One must also note that since the boundary divisors can intersect (transversely, in fact), boundary classes must also be pulled back to moduli spaces to which they do not correspond. We refer the reader to [12] for details.

What remains, then, is to express the Chern classes of the Hodge bundle E in terms of the boundary divisors. This is precisely the content of Mumford's Grothendieck-Riemann-Roch (G-R-R) calculation. Briefly (too briefly!), there is the forgetful map $\rho : \overline{\mathcal{M}}_{g,1} \rightarrow \overline{\mathcal{M}}_{g,0}$ (we now set $\overline{\mathcal{C}} \equiv \overline{\mathcal{M}}_{g,1}$), with respect to which we wish to push forward the relative canonical sheaf $\omega_{\overline{\mathcal{C}}, \overline{\mathcal{M}}}$. Since $\rho_* \omega_{\overline{\mathcal{C}}, \overline{\mathcal{M}}} = E$, the G-R-R formula tells us the Chern character classes of E (we need that $R^1 \rho_* \omega_{\overline{\mathcal{C}}, \overline{\mathcal{M}}} = \mathcal{O}$). The formula calls for integration of $ch(\omega_{\overline{\mathcal{C}}, \overline{\mathcal{M}}})$ with the Todd class of the relative tangent sheaf. The former involves the descendents, while the relative tangent sheaf is dual to the relative cotangent sheaf, which differs from $\omega_{\overline{\mathcal{C}}, \overline{\mathcal{M}}}$ only at the singular locus (on smooth parts, sections of the canonical bundle are just one-forms). The Todd expansion is responsible for the appearance of Bernoulli numbers, while the difference from the canonical sheaf introduces the divisor classes.

Therefore, integrals of descendent classes and λ classes can be performed by using Mumford's formula (see section 1 of [16]) to convert λ classes to descendents and divisor classes, then on the boundaries of $\overline{\mathcal{M}}$ pulling these classes back to the moduli spaces which cover the boundaries. As these spaces have lower genera, the integrals can be performed recursively. Faber has written a computer algorithm in Maple for this procedure, which he generously lent us for this calculation.

2.3. Summing over graphs

The contribution to the free energy $F^{(g)}$ from genus g curves in the class β is given from the fixed point formula as

$$K_\beta^g = \sum_{\Gamma} \frac{1}{|\mathbf{A}_\Gamma|} \int_{\overline{M}_\Gamma} \frac{i^*(\phi)}{e(N^{vir})}, \quad (2.4)$$

with $e(N^{vir})^{-1}$ and $i^*(\phi)$ as described in (2.2)(2.3). The formal expansion of the integrand yields cohomology elements of $\overline{\mathcal{M}}_{g,n}$, the moduli space of pointed curves at the vertices. The integral over \overline{M}_Γ splits into integrals over these moduli spaces, against which the cohomology elements of the right degree have to be integrated. In addition, the contribution of a given graph must be divided by the order of the automorphism group \mathbf{A}_Γ , as we are performing intersection theory in the orbifold sense. \mathbf{A}_Γ contains the automorphism group of Γ as a marked graph and a \mathbf{Z}_{d_e} factor for each edge which maps with degree d_e .

Hence it remains to construct the graphs Γ which label the fixed point loci of $\overline{\mathcal{M}}_{g,k}(d, \mathbf{P}^2)$ under the induced torus action, then to carry out the summation and integration. A graph is labeled by a set of vertices and edges, and can be viewed as a degenerate domain curve with additional data specifying the map to \mathbf{P}^2 . The vertices v represent the irreducible components C_v . They are mapped to fixed points in \mathbf{P}^2 under the torus action. The index of this fixed point $i(v)$ and the arithmetic genus $g(v)$ of the component C_v are additional data of the graph. The edges e represent projective lines which are mapped invariantly, with degree d_e , to projective lines in the toric space connecting the pair of fixed points. A graph without the additional data $g(v), d_e, i(v)$ will be referred to as *undecorated*.

The following combinatorial conditions specify a $\Gamma_{g,d,k}$ graph representing a fixed-point locus of genus g , degree d maps with k marked points:⁶

- (1) if $e \in \text{Edge}(\Gamma)$ connects the vertices (u, v) then $i(u) \neq i(v)$
- (2) $1 - \#(\text{Vertices}) + \#(\text{Edges}) + \sum_{v \in \text{Vert}(\Gamma)} g(v) = g$
- (3) $\sum_{e \in \text{Edge}(\Gamma)} d_e = d$
- (4) $\{1, \dots, k\} = \cup_{v \in \text{Vert}(\Gamma)} S(v)$.

To construct all $\Gamma_{g,d,0}$ graphs we start by generating a list of all possible undecorated graphs that can be decorated to yield $\Gamma_{g,d,0}$ graphs. Hence the number of edges is restricted

⁶ Condition four is relevant only for maps with k marked points, which we do not consider ($k = 0$). $S(v)$ is then the subset of marked points on the component C_v .

by (3) while the number of vertices is restricted by (2). The undecorated graphs with n_v vertices can be represented by an $n_v \times n_v$ symmetric incidence matrix, m . Entries $m_{i,j} = 1$ or 0 represent a link or no link between v_i and v_j , so with a fixed number of edges n_e there will be $\binom{\frac{(n_v+1)n_v}{2}}{n_e}$ possibilities. A main problem is to identify among the graphs those which have different topology. To obtain invariant data, independent of the ordering of the vertices and depending only on the topology of the graph, we use a so called depth-first-search algorithm. This starts with a vertex v_k and descends level-by-level along all occurring branches collecting the data of the encountered vertices, namely the valence (and in later applications the additional information $g(v)$ and $i(v)$ as well as edge data d_α for the map), into a list T_k graded by the level, until all vertices have been encountered. A lexicographic ordering can be imposed on the combined lists of all vertices $T_\Gamma = \{T_1, \dots, T_{n_v}\}$ and $T_{\Gamma_i} = T_{\Gamma_k}$ only if Γ_i is isomorphic to Γ_k . These invariants will be used for a.) generating distinct undecorated graphs, b.) decorating them without redundancy, and c.) finding the automorphism group.⁷ Fig. 1 shows as an example the generation of genus 2, degree 3 graphs.

We have implemented the above generation of graphs⁸ of (2.4) in a completely automated computer algorithm that uses Faber's algorithm to perform the integrals over $\overline{\mathcal{M}}_{g,n}$. We exhibit the results of these localization calculations in the instanton pieces $F_{inst}^{(g)} = \sum_{d>0} K_d^g q^d$ of the partition functions $F^{(g)}$ listed below:

⁷ A useful computer program [17] was used to check the number of undecorated graphs.

⁸ The number of graphs grows very quickly with the genus. E.g., to calculate the $d = 5$ term (for $g = 0, \dots, 5$) in (2.5), one sums over six times 173{21}, 733{101}, 2295{313}, 5353{719}, 11101{1442}, 20345{2570} fully-decorated graphs, where the number in braces indicates the number of graphs with just $g(v)$ and d_e decorations. For example, in the calculation of $(g, d) = (4, 5)$ the maximal dimension of a vertex moduli space $\dim(\overline{\mathcal{M}}_{g,n}) = 14$ occurs in the “star graphs” – irreducible genus 4 curves with five legs. At this dimension, 22462 different 2-d gravity integrands must be evaluated.

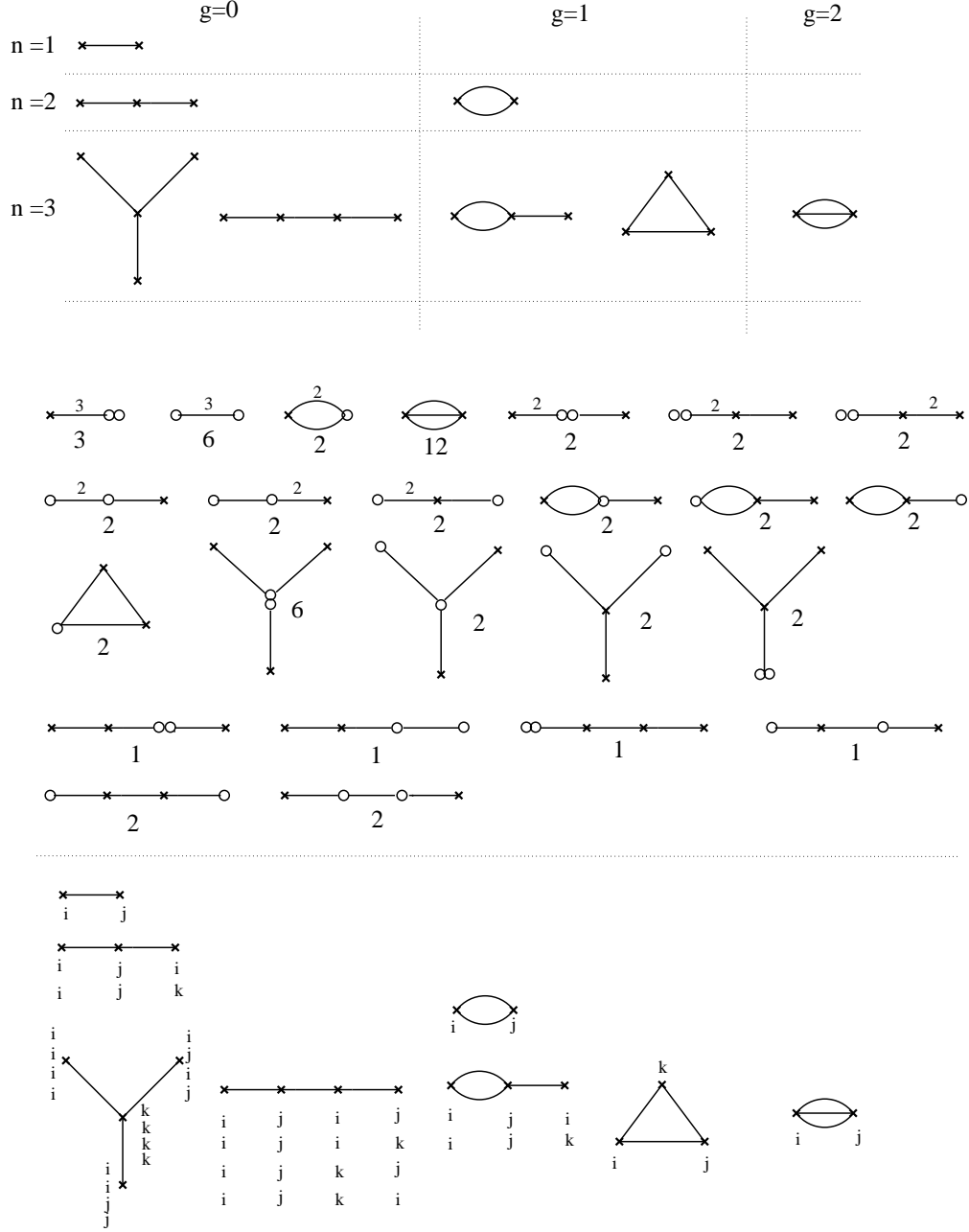


Fig. 1: The first part of the figure shows a scheme of all undecorated graphs that can be decorated to $g = 2$, $d = 3$ graphs. In the middle we show the 24 different ways to decorate them by d_e (small numbers, if different from one) and $g(v)$ (number of circles), with the order of the automorphism \mathbf{A}_Γ indicated by the bigger numbers. In the last part of the figure we show the decoration possibilities by the $i(v)$ indices, which lead to 63 graphs. The indices (i, j, k) are finally summed over all permutations of $(1, 2, 3)$.

$$\begin{aligned}
F^{(0)} &= -\frac{t^3}{18} + 3q - \frac{45q^2}{8} + \frac{244q^3}{9} - \frac{12333q^4}{64} + \frac{211878q^5}{125} \dots \\
F^{(1)} &= -\frac{t}{12} + \frac{q}{4} - \frac{3q^2}{8} - \frac{23q^3}{3} + \frac{3437q^4}{16} - \frac{43107q^5}{10} \dots \\
F^{(2)} &= \frac{\chi}{5720} + \frac{q}{80} + \frac{3q^3}{20} - \frac{514q^4}{5} + \frac{43497q^5}{8} \dots \\
F^{(3)} &= -\frac{\chi}{145120} + \frac{q}{2016} + \frac{q^2}{336} + \frac{q^3}{56} + \frac{1480q^4}{63} - \frac{1385717q^5}{336} \dots \\
F^{(4)} &= \frac{\chi}{87091200} + \frac{q}{57600} + \frac{q^2}{1920} + \frac{7q^3}{1600} - \frac{2491q^4}{900} + \frac{3865234q^5}{1920} \dots \\
F^{(5)} &= -\frac{\chi}{2554675200} + \frac{q}{1774080} + \frac{q^2}{14080} + \frac{61q^3}{49280} + \frac{4471q^4}{22176} - \frac{65308319q^5}{98560} \dots
\end{aligned} \tag{2.5}$$

2.4. Organizing the partition functions

In order to make enumerative predictions from the partition functions, we need the analogue of the multiple-cover formula $(1/k^3)$. In other words, we need to know how a “fundamental object,” a holomorphic curve or D-brane (BPS state) of given charge and spin content, contributes to the partition function.

The functional form of $F^{(g)}$ was derived in [1]:

$$F(\lambda) = \sum_{g=0}^{\infty} F^{(g)} \lambda^{2g-2} = \sum_{\{d_i\}, g \geq 0, k > 0} n_{\{d_i\}}^g \frac{1}{k} (2 \sin \frac{k\lambda}{2})^{2g-2} \exp[-2\pi k \sum_i d_i t_i]. \tag{2.6}$$

Here the $\{d_i\}$ define the homology class (charge) of the BPS state, and $n_{\{d_i\}}^g$ are the number of BPS states of charge $\{d_i\}$ and left-handed spin content described by g .⁹

The table below was generated by extracting the integers from the partition functions as indicated. Results for degrees higher than five come from the B-model calculation, which we review in the next section.

⁹ BPS states are killed by the right-handed supersymmetry generators (half), where $so(4) \cong su(2)_L \otimes su(2)_R$. BPS supermultiplets, formed from a spin (j_1, j_2) Fock “vacuum,” have states with left-handed content $[(\frac{1}{2}) \oplus 2(0)] \otimes j_1$, while the $2j_2 + 1$ right-handed states only contribute an overall factor (with sign). Defining $I = (\frac{1}{2}) \oplus 2(0)$, g labels the representation $I^{\otimes g}$.

d	$g = 0$	$g = 1$	$g = 2$	$g = 3$	$g = 4$
1	3	0	0	0	0
2	-6	0	0	0	0
3	27	-10	0	0	0
4	-192	231	-102	15	0
5	1695	-4452	5430	-3672	1386
6	-17064	80948	-194022	290853	-290400
7	188454	-1438086	5784837	-1536990	29056614
8	-2228160	25301295	-155322234	649358826	-2003386626
9	27748899	-443384578	3894455457	-23769907110	109496290149
10	-360012150	7760515332	-93050366010	786400843911	-5094944994204

Fig. 2: The (weighted) number of BPS states n_d^g for the local \mathbf{P}^2 case.

As an immediate check, we note that $n_d^g = (-1)^{\dim(\mathcal{N}_d)}(d+1)(d+2)/2$ when $g = \binom{d-1}{2}$. In the BPS language, these integers count highest-spin two-brane states with a given charge.¹⁰ The moduli space of polynomials of degree d is $\mathcal{N}_d \equiv \mathbf{P}^{(d+1)(d+2)/2-1}$, and $(d+1)(d+2)/2$ equals the Euler characteristic of this space. A simplification for highest-spin states allows us to ignore the moduli corresponding to bundles on D-branes [1].

If for a given degree d all non-vanishing n_d^g are known, one can reorganize the spin content of BPS states with a fixed charge in the irreducible representations of the left $su(2)_L$. With $n_5^5 = -270$ from (2.5) and $n_5^6 = 21$ for the smooth genus six curve, we get

d	$s = 0$	$s = \frac{1}{2}$	$s = 1$	$s = \frac{3}{2}$	$s = 2$	$s = \frac{5}{2}$	$s = 3$	$s = \frac{7}{2}$
3	4	-13	-10	0	0	0	0	0
4	-27	24	24	18	15	0	0	0
5	78	-57	12	-12	-12	36	24	21

Note that in this basis, the numbers are considerably smaller. It is curious that the next-to-last number in each row is three greater (in absolute value) than the last. Further enumerative remarks are made in section four.

The form (2.6) amounts to a set of multiple-cover formulas which can be found by extracting the appropriate coefficient of λ and k . Let us denote by $C_g(h, d)$ the contribution

¹⁰ This case was first discussed in [18].

of a genus g object in a class β to the partition function at genus $g + h$ in class $d\beta$. From (2.6) we see that $C_g(h, d)$ is the coefficient of $\lambda^{2(g+h)-2}$ in $d^{-1}(2 \sin(d\lambda/2))^{2g-2}$. Some of these numbers have been corroborated by mathematical calculations. For example, $C_0(0, d) = 1/d^3$ [19][20]. $C_0(h, d)$ was calculated in [16], and $C_g(h, 1), g \geq 1$ in [21]. R. Pandharipande has communicated to us another subtraction scheme when $h = 0$ which also yields integers.

A puzzle remains, however. The multiple-cover formulas predict, for example, that genus two objects of degree four contribute to the partition function at genus two, degree eight. However, no double covers of genus two curves by genus two curves are expected. In general, since no covering maps from genus g to $g + h$ curves exist, how does one even *define* the covering contribution? Perhaps a formulation via spaces of sheaves (which we discuss in section four) is in order.

2.5. Example

For example, the coefficient $K_4^2 = -514/5$ of q^4 in $F^{(2)}$ in (2.5) can receive contributions from the non-zero integer invariants $n_1^0, n_2^0, n_4^0, n_4^1$, and n_4^2 . Since $C_0(2, d) = d/240$, $C_1(1, d) = 0$, and $C_2(0, d) = d$, we see

$$K_4^2 = 3(4/240) - 6(2/240) - 192(1/240) + 231(0) - 102(1) = -514/5.$$

3. B-Model Calculations

Though [4] developed recursion relations for Calabi-Yau threefolds, the lesson of [2] is that considerations involving holomorphic curves inside Fano subvarieties within Calabi-Yau threefolds may be isolated to calculations on the canonical bundle qua normal bundle of the surface. The reason for this is that all curves within the surface have negative self-intersection and so can't be moved off of the surface. The topological partition functions count holomorphic curves of higher genus, in some sense, so we expect to find a “local” version of the equations of Kodaira-Spencer gravity, developed in [3][4]. We will now describe the simplifications in the Kodaira-Spencer theory as we specialize to the local case.

3.1. The vacuum line bundle and correlation functions

In $N = 2$ topological theories the vacuum state $|0\rangle$ transforms as a section of a holomorphic line bundle \mathcal{L} over the moduli space \mathcal{M} of the theory. In the case of the B-type topological σ -models, the former will be identified with the holomorphic $(3,0)$ -form Ω while \mathcal{M} will be identified with the complex structure moduli space of the Calabi-Yau geometry \hat{X} , which is mirror dual to the geometry X on which we count the holomorphic maps. \mathcal{M} has a special Kähler structure, with Kähler potential $K(z, \bar{z})$.

By the sewing axioms of topological field theory the vacuum amplitudes at genus g $F^{(g)}$ are sections of \mathcal{L}^{2-2g} over \mathcal{M} . The general topological correlations function $F_{i_1 \dots i_n}^{(g)} \in \mathcal{L}^{2-2g} \otimes \text{Sym}_n T^* \mathcal{M}$ are defined as covariant derivatives of the “potentials” $F^{(g)}$ as $F_{i_1 \dots i_n}^{(g)} = D_{i_1} \dots D_{i_n} F^{(g)}$. The D_i are covariant with respect to metric connection $\Gamma_{lk}^i = G^{i\bar{m}} \partial_l G_{k\bar{m}}$ of the Weil-Peterson-Zamolodchikov metric $G_{k\bar{l}}(z, \bar{z}) = \partial_k \bar{\partial}_{\bar{l}} K$ on \mathcal{M} as well as the Kähler connection $A_i = \partial_i K$ of the line bundle \mathcal{L} .

3.2. The key holomorphic object at genus zero: $F_{i_1, i_2, i_3}^{(0)}$

The genus zero three-point functions $F_{i_1, i_2, i_3}^{(0)}$, physically well-known as the Yukawa couplings of the heterotic string with standard embedding or the magnetic moments in the type-II compactifications, are of special importance because, as their moduli space has no boundaries, they are truly holomorphic and appear as building blocks in the recursive definition of the higher loop amplitudes.

They can be explicitly calculated as integrals over the Calabi-Yau manifold \hat{X}

$$F_{i_1, i_2, i_3}^{(0)}(z) = - \int_{\hat{X}} \Omega \partial_{z_{i_1}} \partial_{z_{i_2}} \partial_{z_{i_3}} \Omega \quad (3.1)$$

which can be expressed as the derivatives of suitable combinations of period integrals over the cycles of \hat{X} . These period integrals can be most easily reconstructed from solutions of the Picard-Fuchs system of \hat{X} . For the local case, the $F_{i_1, i_2, i_3}^{(0)}$ can be defined either as a limit of a global Calabi-Yau geometry or intrinsically from the Picard-Fuchs system for the local geometry. We sometimes write $C_{i,j,k}$ for $F_{i,j,k}^{(0)}$.

3.3. The canonical coordinates t_i and the holomorphic limit

Other correlation functions $F_{i_1, \dots, i_r}^{(g)}$ for $g > 0$ are not holomorphic.¹¹ However, due to a uniquely distinguished class of coordinate systems on \mathcal{M} , the *canonical* coordinates, there is a well-defined limit one can take to define holomorphic correlators.

Of the $2h^{2,1} + 2 = 2\dim(\mathcal{M}) + 2$ period integrals $\omega_i = \int_{\gamma_i} \Omega$, near the maximal unipotent point $P_M = (z_i = 0, \text{Im}(t_i) \rightarrow \infty) \in \mathcal{M}$, exactly $h^{2,1}$ will have logarithmic behavior $\omega_i \sim \log(z_i) + O(z)$, $i = 1, \dots, h^{2,1}$. A unique one $\omega_0 = 1 + O(z)$ is analytic. The homogeneous coordinates, defined as $2\pi i t_i = \frac{\omega_i}{\omega_0} \sim \log(z_i)$, have the following properties, which define canonical coordinates near any point P_0 .

All holomorphic derivatives vanish at P_0

$$\partial_{t_1} \dots \partial_{t_r} \Gamma_{ij}^k|_{P_0} = 0, \quad \partial_{t_1} \dots \partial_{t_r} K|_{P_0} = 0. \quad (3.2)$$

Let as above P_0 be at $z = 0$, $t = t_0$. Then (3.2) implies that in the t coordinates the leading term in $\bar{\lambda}_i = (\bar{t}_i - \bar{t}_0)$ of $K = C + O(\bar{\lambda})$ and $G_{i\bar{j}} = C_{i,\bar{j}} + O(\bar{\lambda})$ is constant. When re-expressed in the coordinates z_i , the holomorphic parts of K and G in the $\bar{\lambda}_i \rightarrow 0$ limit are

$$K = C - \log(\omega_0), \quad G_{i\bar{m}} = \frac{\partial t_k}{\partial z_i} C_{k\bar{m}}. \quad (3.3)$$

In all quantities to be discussed below we will take the holomorphic $\bar{\lambda} \rightarrow 0$ limit.

The t_i at P_M have the additional property that they are identified by mirror symmetry with the complexified Kähler parameters of the mirror X , and the $F_{i_1, \dots, i_r}^{(g)}$ are curve-counting functions for holomorphic maps of genus g into X . Note also that t_i at P_M are the special coordinates in which the holomorphic parts of the Kähler connection and the Weil-Peterson connection vanish, i.e. D_i becomes the ordinary derivative ∂_{t_i} .

At this point there is important simplification in the local case. As is clear from the differential equations associated to the local case [22][2], $\omega_0 = 1$ is always a holomorphic solution, and hence for the local case the holomorphic part of the Kähler potential becomes trivial in the limit (3.3).

¹¹ Note that $F_{i_1, \dots, i_n}^{(0)}$ for $n = 0, 1, 2$, may have an anti-holomorphic dependence.

3.4. The holomorphic anomaly at genus one and the derivation of $F^{(1)}$

The genus one topological partition function is defined as

$$F^{(1)} = \frac{1}{2} \int_{\mathcal{F}} \frac{d^2\tau}{\text{Im}(\tau)} \text{Tr}_{\text{Ra}, \overline{\text{Ra}}} (-1)^F F_L F_R q^{H_L} \bar{q}^{H_R} . \quad (3.4)$$

Note that without the insertions of the left and right fermion number operators, the integrand would be the Witten index and just receive contributions from the ground states $\text{Tr}(-1)^F = \chi$. The holomorphic anomaly due to contributions from the boundary of the moduli space was derived in [3] for general $N = 2$ theories and specializes for the $\hat{c} = 3$ case to¹²

$$\partial_i \bar{\partial}_{\bar{j}} F^{(1)} = \frac{1}{2} F_{ijk}^{(0)} \bar{F}_{\bar{j}\bar{k}\bar{l}}^{(0)} e^{2K} G^{j\bar{k}} G^{k\bar{l}} - \left(\frac{\chi}{24} - 1 \right) G_{i\bar{j}} . \quad (3.5)$$

Using $R_{i\bar{j}} = -\frac{1}{2} \frac{\partial^2 \log \det(G)}{\partial_i \partial_{\bar{j}}}$ and the special geometry relation

$$R_{i\bar{j}l}^k = G_{i\bar{j}} \delta_l^k + G_{l\bar{j}} \delta_i^k - F_{ilm}^{(0)} \bar{F}_{\bar{j}\bar{p}\bar{q}}^{(0)} e^{2K} G^{k\bar{p}} G^{m\bar{q}} , \quad (3.6)$$

one can integrate (3.5) up to an unknown holomorphic function f to yield

$$F^{(1)} = \log \left(\det(G^{-1})^{\frac{1}{2}} e^{\frac{K}{2}(3+h^{2,1}-\frac{1}{12}\chi)} |f^2| \right) . \quad (3.7)$$

The holomorphic ambiguity f can be parameterized by the vanishing or pole behavior at the discriminant loci $f = \prod_{i=1}^k (\Delta_k)^{r_i} \prod_{i=1}^{h^{2,1}} z_i^{x_i}$. In particular, the x_i can all be determined by the limiting behavior $\lim_{z_i \rightarrow 0} F^{(1)} = -\frac{1}{24} \sum_{i=1}^{h^{2,1}} t_i \int_X c_2 J_i$. The behavior of $F^{(1)}$ at certain types of singularities is universal – e.g., for the conifold singularity $r_{con} = -\frac{1}{12}$. By virtue of the remark at the end of the previous section, χ and $h^{1,2}$ only affect an irrelevant additive constant to $F^{(1)}$ in the local case. Note that on the other hand, the topological number $\int_X c_2 J_i$ is crucial for fixing the large t_i behaviour of $F^{(1)}$ in the local case. Formulas for $\int_X c_2 J_i$ in the local case can be found in [2].

¹² The normalization of $F^{(1)}$ in [3] is by a factor 2 greater than the one in [4]. We will adopt the latter.

3.5. The higher genus anomaly and the derivation of the $F^{(g)}$

The higher genus correlators are defined by a recursive procedure using the holomorphic anomaly equation

$$\begin{aligned} \bar{\partial}_{\bar{i}} F_{i_1, \dots, i_n}^{(g)} &= \frac{1}{2} \bar{C}_{\bar{i}}^{jk} F_{jk i_1, \dots, i_n}^{(g-1)} + \\ &\frac{1}{2} \bar{C}_{\bar{i}}^{jk} \sum_{r=0} \sum_{s=0} \frac{1}{s!(n-s)!} \sum_{\sigma \in S_n} F_{j i_{\sigma(1)} \dots i_{\sigma(s)}}^{(r)} F_{k i_{\sigma(s+1)} \dots i_{\sigma(n)}}^{(g-r)} \\ &- (2g - 2 + n - 1) \sum_{s=1}^n G_{\bar{i}, i_s} F_{i_1 \dots i_{s-1} i_{s+1} \dots i_n}^{(g)}, \end{aligned} \quad (3.8)$$

where $\bar{C}_{\bar{i}}^{ij} \equiv \bar{F}_{i\bar{j}\bar{k}}^{(0)} e^{2K} G^{j\bar{j}} G^{k\bar{k}}$. The right-hand side corresponds to the boundary contributions of the moduli space of marked Riemann surfaces, $\overline{\mathcal{M}}_{g,n}$. The first term comes from pinching a handle, the next from splitting the surface into two components by growing a long tube, the last from when the insertion approaches marked points.

The solution of the equation is provided by the calculation of potentials for the non-holomorphic quantities $\bar{C}_{\bar{i}}^{ij}$. In the first, step one calculates $S^{ij} \in \mathcal{L}^{-2} \otimes \text{Sym}_2 T\mathcal{M}$ such that $\bar{C}_{\bar{i}}^{ij} = \bar{\partial}_{\bar{i}} S^{ij}$. This follows from (3.6) by noting that in Kähler geometry $R_{i\bar{j}l}^k = -\bar{\partial}_{\bar{j}} \Gamma_{il}^k$, and hence

$$\bar{\partial}_{\bar{k}}[S^{ij} C_{jkl}] = \bar{\partial}_{\bar{k}}[\delta_l^i \partial_k K + \delta_k^i \partial_l K + \Gamma_{kl}^i] . \quad (3.9)$$

The derivatives $\bar{\partial}_{\bar{k}}$ on both sides can be removed at the price of introducing a meromorphic object f_{kl}^i , which also has to compensate the non-covariant transformation properties of quantities on the right-hand side.

Therefore it is natural to split f_{kl}^i into quantities with simple transformation properties: $f_{kl}^i = \delta_k^i \partial_l \log f + \delta_l^i \partial_k \log f - v_{l,a} \partial_k v^{i,a} + \tilde{f}_{kl}^i$, where \tilde{f}_{kl}^i now transforms covariantly, $f \in \mathcal{L}$, and $v^{i,a}$ transform as tangent vectors. The choices of the f , $v^{i,a}$, \tilde{f}_{kl}^i are by no means independent, however. If we specialize to the one-modulus case, as in our main example the local \mathbf{P}^2 , we can in addition set $\tilde{f}_{zz}^z = 0$ and in the holomorphic limit get the simplified expression

$$\begin{aligned} S^{zz} &= \frac{1}{F_{zzz}^{(0)}} [2\partial_z \log(e^K |f|^2) - (G_{z\bar{z}} v)^{-1} \partial_z (v G_{z\bar{z}})] \\ &= -\frac{1}{F_{zzz}^{(0)}} \partial_z \log \left(v \frac{\partial t}{\partial z} \right) \quad \text{as } \bar{\lambda} \rightarrow 0, \end{aligned} \quad (3.10)$$

where $v \in T\mathcal{M}$ to render S^{zz} covariant. The simplification in the second line is due to the fact that K is constant in the holomorphic limit for the local case and f can be chosen to be

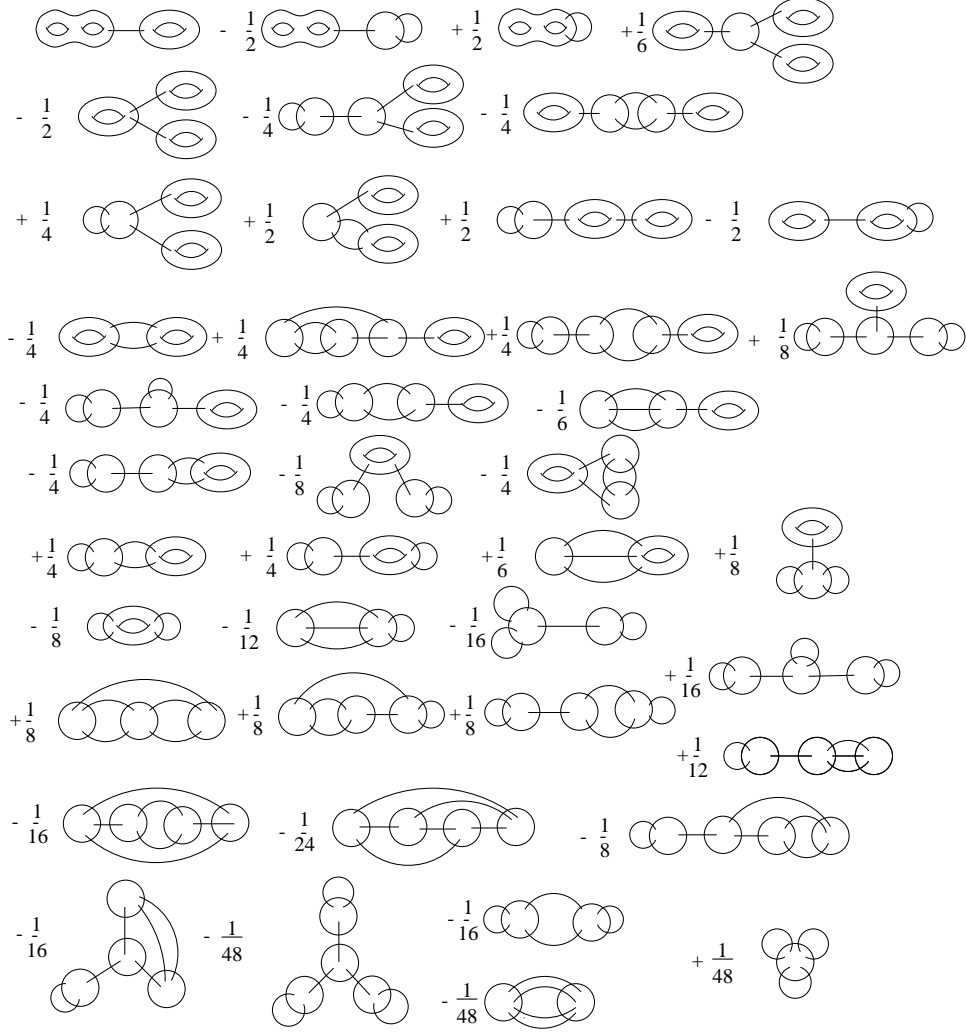


Fig. 3: The degenerations of a genus 3 Riemann surface, with the symmetry factors by which they contribute to the calculation of $F^{(3)}$. In the local case, these are all the contributions. The diagrams correspond (in order) to terms in the expression for $F^{(3)}$, though one expression may involve several graphs. For example, the fifth line in the figure contains the three graphs which contribute to $-\frac{2}{3}S_2^4 F_{,1}^{(1)} F_{,4}^{(0)} F_{,3}^{(0)}$. Lines denote factors of S_2 , genus g components with valence n represent factors of $F_n^{(g)}$. In the global case, there are 81 additional graphs with ϕ propagators.

constant as well. Further potentials needed to solve for the $F^{(g)}$ in the global cases are $S \in \mathcal{L}^{-2}$, with $C_{\bar{j}\bar{k}\bar{l}} = e^{-2K} D_{\bar{i}} D_{\bar{j}} \bar{\partial}_{\bar{k}} \bar{S}$, $S_{\bar{i}} \equiv \bar{\partial}_{\bar{i}} S$, $\bar{\partial}_{\bar{i}} S^j = G_{i\bar{i}} S^{ij}$. $K^{ij} = -S^{ij}$, $K^{i\phi} = -S^i$ and $K^{\phi\phi} = -2S$ can be interpreted as propagators in the topological gravity theory, where ϕ is the dilaton, the first descendent of the puncture operator. However, in the local case we will see that a choice of the different holomorphic ambiguities can be made so that $K^{i\phi}$

and $K^{\phi\phi}$ vanish. S^i is derived from

$$\bar{\partial}_{\bar{z}} S^z = \frac{1}{F_{zzz}^{(0)}} \bar{\partial}_{\bar{z}} [2\partial_z \log(e^K |f|^2)^2 - v^{-1} \partial_z (v \partial_z K)] ,$$

and if we set the holomorphic ambiguity in the special solution to this equation to zero, it vanishes in the holomorphic limit for the local case. Similarly one can see that S vanishes.

The derivation of $F^{(g)}$ proceeds recursively. One first considers the holomorphic anomaly equation of $F^{(g)}$, and using $\bar{C}_i^{ij} = \bar{\partial}_i S^{ij}$, one can write the right-hand side e.g. for $g = 2$ as $\frac{1}{2} \bar{\partial}_i [S^{jk} (F_{jk}^{(1)} + F_j^{(1)} F_k^{(1)})] - \frac{1}{2} S^{jk} \bar{\partial}_i [F_{jk}^{(1)} + F_j^{(1)} F_k^{(1)}]$. Using the definition of the Riemann tensor as commutator and special geometry, i.e. $[\bar{\partial}_i, D_j]_k^l = -G_{ij} \delta_k^l - G_{ik} \delta_j^l + C_{jkm} \bar{C}_i^{ml}$, one lets the $\bar{\partial}_i$ derivative act on $F^{(g-1)}$ and repeats the procedure until an expression $\bar{\partial}_i F^{(g)} = \bar{\partial}_i [\dots]$ is derived, where $[\dots]$ contains the propagators and lower-genus correlation functions.

This yields, again up to holomorphic ambiguity at every final integration step,

$$\begin{aligned} F^{(2)} = & -\frac{1}{8} S_2^2 F_{,4}^{(0)} + \frac{1}{2} S_2 F_{,2}^{(1)} + \frac{5}{24} S_2^3 (F_{,3}^{(0)})^2 - \frac{1}{2} S_2^2 F_{,1}^{(1)} F_{,3}^{(0)} + \frac{1}{2} S_2 (F_{,1}^{(1)})^2 + f^{(2)} \\ F^{(3)} = & S_2 F_{,1}^{(2)} F_{,1}^{(1)} - \frac{1}{2} S_2^2 F_{,1}^{(2)} F_{,3}^{(0)} + \frac{1}{2} S_2 F_{,2}^{(2)} + \frac{1}{6} S_2^3 (F_{,1}^{(1)})^3 F_{,3}^{(0)} - \frac{1}{2} S_2^2 F_{,2}^{(1)} (F_{,1}^{(1)})^2 \\ & - \frac{1}{2} S_2^4 (F_{,1}^{(1)})^2 (F_{,3}^{(0)})^2 + \frac{1}{4} S_2^3 (F_{,1}^{(1)})^2 F_{,4}^{(0)} + S_2^3 F_{,2}^{(1)} F_{,1}^{(1)} F_{,3}^{(0)} - \frac{1}{2} S_2^2 F_{,3}^{(1)} F_{,1}^{(1)} \\ & - \frac{1}{4} S_2^2 (F_{,2}^{(1)})^2 + \frac{5}{8} S_2^5 F_{,1}^{(1)} (F_{,3}^{(0)})^3 - \frac{2}{3} S_2^4 F_{,1}^{(1)} F_{,4}^{(0)} F_{,3}^{(0)} - \frac{5}{8} S_2^4 F_{,2}^{(1)} (F_{,3}^{(0)})^2 \\ & + \frac{1}{4} S_2^3 F_{,2}^{(1)} F_{,4}^{(0)} + \frac{5}{12} S_2^3 F_{,3}^{(1)} F_{,3}^{(0)} + \frac{1}{8} S_2^3 F_{,5}^{(0)} F_{,1}^{(1)} - \frac{1}{8} S_2^2 F_{,4}^{(1)} - \frac{7}{48} S_2^4 F_{,5}^{(0)} F_{,3}^{(0)} \\ & + \frac{25}{48} S_2^5 F_{,4}^{(0)} (F_{,3}^{(0)})^2 - \frac{5}{16} S_2^6 (F_{,3}^{(0)})^4 - \frac{1}{12} S_2^4 (F_{,4}^{(0)})^2 + \frac{1}{48} S_2^3 F_{,6}^{(0)} + f^{(3)} , \end{aligned}$$

where $S_2 \equiv S^{zz}$ and $F_{,n}^{(g)} \equiv (D_z)^n F^{(g)}$.

Notice that in the local case the χ drops out, as expected. These terms represent the various degenerations of the genus g Riemann surface, and it is useful to keep track of the calculation by interpreting them as Feynman rules for the auxiliary finite quantum system. Clearly the symmetry factors are of the utmost importance to the calculation. We exhibit these and all 41 diagrams which contribute in the local limit to $F^{(3)}$ in Fig. 3.

3.6. The local \mathbf{P}^2 case

\mathbf{P}^2 is torically defined by the integral lattice polyhedron $\Sigma = \text{conv}\{(-1, -1), (1, 0), (0, 1)\}$. The non-compact A-model geometry¹³ $\mathcal{O}(-3) \rightarrow \mathbf{P}^2$ is torically described by a fan spanned by $\{(1, -1, -1), (1, 1, 0), (1, 0, 1)\}$. By the mirror construction of [24] applied to the local case [22], the mirror B-model geometry follows then from the periods of a meromorphic differential λ on the Riemann surface described by the vanishing of the $(1, 1)$ -shifted Newton polynomial associated to the dual polyhedron $\Sigma^* = \text{conv}\{(-1, -1), (2, -1), (-1, 2)\}$. In this case, we simply have a cubic $P = x_1^3 + x_2^3 + x_3^3 - 3\psi x_1 x_2 x_3 = 0$ in $\mathbf{P}^2 = \mathbf{P}_{\Sigma^*}$.

Differential equations for the periods of λ in the mirror geometry follow from the \mathbf{C}^* scaling actions on the local A-model geometry. As described in [22] these translate directly into Picard-Fuchs differential operators, which in the \mathbf{P}^2 case gives¹⁴

$$\mathcal{L} = \theta^3 - x \prod_{i=1}^3 (\theta - a_i + 1) = \tilde{\mathcal{L}}\theta, \quad a_1 = \frac{1}{3}, \quad a_2 = \frac{2}{3}, \quad a_3 = 1, \quad (3.11)$$

where $\theta = x \frac{d}{dx}$. This is the defining equation for the Meijer G-function $G_{3,3}^{2,2} \left(-x \middle| \begin{smallmatrix} a_1 a_2 a_3 \\ 0 \ 0 \ 0 \end{smallmatrix} \right)$, which we denote $G(a_1, a_2, a_3; x)$ for short [25].¹⁵

To find the solutions to (3.11) which correspond to actual integrals of λ over cycles, we relate them to the periods over the vanishing cycles. Both periods (apart from the trivial residue) are fixed up to an overall normalization by the Lefschetz theorem on vanishing cycles:

- $t_d = \frac{\partial \mathcal{F}}{\partial t}$ from the logarithmic solution $t_d \log(1 - 27z) + \text{hol. at } z = \frac{1}{27}$.
- $t = \sigma_0 \log(z) + \sigma_2$ from the double-logarithmic solution at the large complex structure limit $z = 0$: $\log(z)(\sigma_0 \log(z) + 2\sigma_1)$, where σ_0 has no constant term.

¹³ A simple global Calabi-Yau, in which this geometry is embedded, is e.g. defined by the vanishing locus of a degree 18 polynomial in $\mathbf{P}^4(1, 1, 1, 6, 9)$. Using mirror symmetry some Gromov-Witten invariants for this space have been calculated [23].

¹⁴ Here we have set $x = 27z = 1/\psi^3 = 27(-1/a_0^3)$ (in comparison with [2]) to bring the singularities to $0, 1, \infty$.

¹⁵ This function is the logarithmic integral $\frac{\Gamma(a_1)\Gamma(a_2)}{\Gamma(a_3)} \int \frac{dx}{x} {}_2F_1$ of the hypergeometric function ${}_2F_1(a_1, a_2; a_3, x)$ solving $\tilde{\mathcal{L}}$. Solutions $\tilde{\omega}_i$ of $\tilde{\mathcal{L}}$ are related to the periods of $P = 0$, $\omega_i = \int_{\gamma_i} \Omega$ with $\Omega = \frac{dx}{y}$, by $\omega_i = \frac{\tilde{\omega}_i}{\psi}$. To check this one may use the Weierstrass form of the $\Gamma(3)$ curve $P = 0$ $y^2 = 4x^3 - xg_2 - g_3$ with $g_2 = 3\psi(8 + \psi^3)$, $g_3 = 8 + 20\psi^3 - \psi^6$. The general theory of Picard-Fuchs equations for elliptic curves then gives for ω_i the differential equation $(\psi^3 - 1)\omega'' + 3\psi^2\omega' + \psi\omega = 0$, the same as that which follows from $\tilde{\mathcal{L}}(\psi\omega) = 0$.

It turns out that $t(x) = i \frac{\Gamma(a_3)}{2\pi\Gamma(a_1)\Gamma(a_2)} G(a_1, a_2, a_3; x)$ is precisely the mirror map¹⁶ and t_d follows by analytic continuation of the vanishing period at $x = 1$ to produce at $z = 0$ the basis of periods

$$\begin{pmatrix} \frac{\partial \mathcal{F}}{\partial t_i} \\ 1 \\ t_i \end{pmatrix} = \begin{pmatrix} -\frac{d_{ijk}}{2} t_i t_k + a_{ik} t_k + \frac{1}{24} c_2 J_i + O(q) \\ 1 \\ t_i \end{pmatrix} \quad (3.12)$$

with $d = -\frac{1}{3}$, $a = -\frac{1}{6}$ and $c_2 J = -2$ as expected from the local limit. Here we have chosen a normalization¹⁷ of t_d such that the derivative $\partial_t^3 \mathcal{F}$ of the period which stays finite in the local limit, $\frac{\partial \mathcal{F}}{\partial t} = -\frac{1}{3}(\partial_{t_E} - 3\partial_{t_B})$, reproduces C_{ttt} . This choice is also natural in the sense that the value of $c_2 J = -2$ reproduces the leading behavior of $F_{top}^{(1)} = \frac{c_2 J}{12} t + \dots$

With this normalization and $u = 1 - x$, one has near $u = 0$:

$$\begin{aligned} 2\pi i t_d &= A u + \text{higher order}, \\ 2\pi i t &= 2\pi i t(1) + B u + C u \log u + \text{higher order}, \end{aligned} \quad (3.13)$$

with $A = 3^{-3/2} i$, $B = i \frac{(\log(27)+1)\sqrt{3}}{(2\pi)}$, $C = \frac{\sqrt{3}}{(2\pi)}$.

At this point, we can use the three-point functions to solve the \mathbf{P}^2 topological partition functions at higher-genus as we have outlined in this section. We will use this analysis to investigate the asymptotic growth of the n_d^0 in the next section. The numerical invariants extracted from these higher-genus calculations were listed in Fig. 2. These B-model calculations yield results for very high degree, though adding genera requires fixing the holomorphic ambiguity.

Solving the B-model recursion relations gives the topological partition functions. As with knowing the prepotential in (genus zero) mirror symmetry, this is not enough to make enumerative predictions. First one needs to find the Kähler parameters t_i (the “mirror map”). In the present case, the mirror map states that the Kähler parameter t is equal to the logarithmic solution of the Picard-Fuchs equation (3.11) of the local geometry (no ratio is needed since the holomorphic solution is constant). Then one must organize the

¹⁶ The implicit choice of the constant term $\log(27)$ fits the definition of the mirror map, a fact which turns out to be right for all local mirror symmetry systems whose Picard-Fuchs equation is Meijer’s equation.

¹⁷ If we simply take the limit of the 3-fold periods, the normalization of t_d differs from this choice by -3 .

prepotential according to (2.6), as outlined in section 2.4, to account for multiple-cover contributions. The result is an expansion in terms of integer coefficients $n_{\{d_i\}}^g$.

Of course, this process demands that the ambiguity (the holomorphic section $f^{(g)}$) at each step in the recursion be fixed. There are $2g - 1$ unknowns in this function, which we fix by matching Gromov-Witten invariants for the first $2g - 1$ degrees at genus g .

There is another way to fix one of these coefficients. Ghoshal and Vafa argue in [26] that the leading coefficient of the ambiguity $f^{(g)}$ at the conifold singularity is determined by the free energy of the $c = 1$ string evaluated at the self-dual radius. Recall that $f^{(g)}$ has the form $\sum_{k=0}^{2g-2} A_k^{(g)} u^{-k}$, where the conifold is at $u = 0$.¹⁸ It turns out that the leading behavior of $F^{(g)}$ is determined by $A_{2g-2}^{(g)}$ alone, as the other terms both in the anomaly and from the recursion have subleading contributions. Ghoshal and Vafa's identification then gives

$$A_{2g-2}^{(g)} = \frac{B_{2g}}{2g(2g-2)},$$

where the B_{2g} are Bernoulli numbers. We should comment that as $f^{(g)}$ is a section of the vacuum line bundle \mathcal{L} , this equation only makes sense in a certain gauge. One can use the $g = 0$ contribution to fix the gauge, then determine the higher $A_{2g-2}^{(g)}$. Note that the independent determination of the ambiguity via localization calculations gives a corroboration of this formula at $g = 2, 3$. In Fig. 2, the entries $n_{d \geq 6}^4$ rely on this procedure.

This is how Fig. 2 was derived from the B-model.

4. Some Enumerative Issues

The holomorphic curves that these numbers count are not simply worldsheet instantons. As shown by Vafa and Gopakumar [1], they represent D-branes in type-II or M-theory compactifications. In this section, we will analyze the growth of these invariants at genus zero, then make some remarks regarding a proper mathematical interpretation of the integers.

¹⁸ Ghoshal and Vafa employ a double-scaling limit $\lambda \rightarrow 0$ and $u \rightarrow 0$ with λ/u fixed, where λ is the string coupling. This isolates the leading behavior of $F^{(g)}$ from the subleading terms in $F^{(g+h)}$.

4.1. Asymptotic growth of states

Let us return now to the solutions (3.13) of the \mathbf{P}^2 period equations.

The singularity at $x = 1$ limits the radius of convergence of the instanton expansion and in particular the exponential growth of $|n_d|$ must be $e^{2\pi t_2(1)}$, where $t_2 = \text{Im}(t)$. For an interpretation of the $n_d \equiv n_d^0$ as BPS counts for some physical system, the logarithm of the multiplicity of the BPS states is the entropy in the large d limit and an important critical exponent of the theory. The value

$$t(1) = \frac{i}{2\pi\Gamma(\frac{1}{3})\Gamma(\frac{2}{3})} G\left(\frac{1}{3}, \frac{2}{3}, 1; 1\right) \sim -\frac{1}{2} + i \, 0.462757788\dots, \quad (4.1)$$

is therefore of particular interest. The real part $\frac{1}{2}$ means that the n_d come with alternating sign. Fig. 4 shows how the logarithmic slope of $|n_d|$ approaches $t_2(1) = \text{Im}(t(1))$.

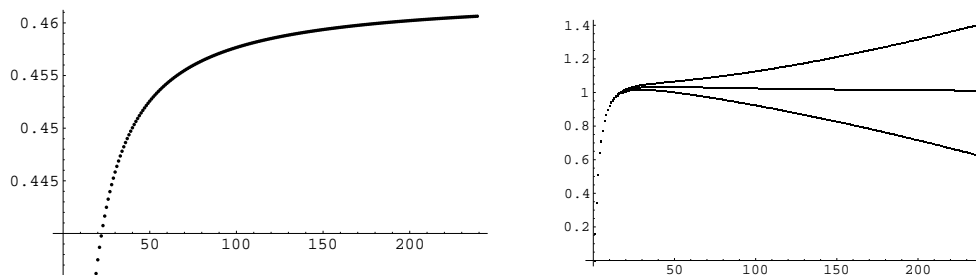


Fig. 4: Left: the slope of $\frac{\log(|n_d|)}{2\pi}$ for $d = 1, \dots, 240$ approaches $t_2(1)$ for high d . Right: Sensitivity of the third Richardson transform of n_d/n_d^{asymp} on $t_2(1)$. The curve approaching 1 is for correct $t_2(1)$ value (4.1) the lower/upper curve is for $t_2(1) \pm \varepsilon$ with $\varepsilon = 2 \times 10^{-6}$.

More precisely, one can also determine as in [27] the first subleading logarithms by comparing the ansatz for $n_d^{asymp} \sim N d^\rho \log(d)^\sigma e^{2\pi d t_2(1)}$ in the asymptotic expansion with C_{uuu} . The Yukawa coupling in the x variable

$$F_{xxx}^{(0)} = -\frac{1}{3(2\pi i)^3} \frac{1}{x^3(1-x)} \quad (4.2)$$

is normalized so that that $F_{ttt}^{(0)} = \left(\frac{dz}{dt}\right)^3 F_{zzz}^{(0)} = -\frac{1}{3} + \sum_{d=1} \frac{d^3 n_d q^d}{1-q^d}$ reproduces the genus 0 instantons as in Fig. 2. This and the knowledge of the $u \log u$ coefficient in the $t(u)$ expansion yields

$$n_d^{asymp} \sim \frac{-\int J^3}{C^2} \frac{e^{-2\pi i d t(1)}}{d^3 \log(d)^2}. \quad (4.3)$$

Instead of just comparing n_d/n_d^{asym} one can suppress further subleading logarithms by considering higher order Richardson transforms [27], which also approach one. This gives a far more sensitive check on the $t_2(1)$ slope from the instanton numbers – see Fig. 4.

The formula (4.1) describes the asymptotic of other one-modulus local mirror symmetry systems with Picard-Fuchs equations given by Meijer's equation with solution $G(a_1, a_2, a_3; x)$. These cases were discussed in [28][29][2]. If we define $b \equiv b(\vec{a}) \equiv 2\Psi(a_3) - \Psi(a_1) - \Psi(a_2)$ (here $\Psi(x) = d(\log \Gamma(x))/dx$ is the digamma function), then we have:

- $(\frac{1}{2}, \frac{1}{2}, 1)$: describes the diagonal direction in $\mathbf{P}^1 \times \mathbf{P}^1$ with $x = e^b z$ [2] as well as a direction in the E_5 del Pezzo, with $x = -e^b z$.
- $(\frac{1}{3}, \frac{2}{3}, 1)$: describes \mathbf{P}^2 as discussed, with $x = e^b z$, as well as a direction in the E_6 del Pezzo, with $x = -e^b z$.
- $(\frac{1}{4}, \frac{3}{4}, 1)$: describes a direction in the E_7 del Pezzo, with $x = -e^b z$.
- $(\frac{1}{6}, \frac{5}{6}, 1)$: describes a direction in the E_8 del Pezzo, with $x = -e^b z$.

With $B(\vec{a}) \equiv i \frac{b(\vec{a})+1}{2\pi}$ we summarize some of their relevant properties, which follow to a large extent from Meijer's fundamental system of solutions.

	$\int J^3$	$\int c_2 J$	a	A	B	C	$t(1)$	Γ
$P^1 \times P^1$	-1	2	0	$-\frac{i}{2}$	$2B(\vec{a})$	$\frac{1}{\pi}$	$.371226 i$	$\Gamma^0(4)$
E_5	-4	$-^*4$	$-\frac{4}{2}$	$-\sqrt{4}i$	$\sqrt{4}B(\vec{a})$	$\frac{1}{\pi}$	$-\frac{1}{2} + .371226 i$	$\Gamma_0(4)$
P^2	$-\frac{1}{3}$	-2	$-\frac{1}{6}$	$\frac{i}{3^{3/2}}$	$\sqrt{3}B(\vec{a})$	$\frac{\sqrt{3}}{2\pi}$	$-\frac{1}{2} + .462757 i$	$\tilde{\Gamma}^0(3)$
E_6	-3	$-^*6$	$-\frac{3}{2}$	$i\sqrt{3}$	$\sqrt{3}B(\vec{a})$	$\frac{\sqrt{3}}{2\pi}$	$-\frac{1}{2} + .462757 i$	$\Gamma_0(3)$
E_7	-2	-8	$-\frac{2}{2}$	$-i\sqrt{2}$	$\sqrt{2}B(\vec{a})$	$\frac{\sqrt{2}}{2\pi}$	$-\frac{1}{2} + .610262 i$	$\Gamma_0(2)$
E_8	-1	-10	$-\frac{1}{2}$	$-i$	$B(\vec{a})$	$\frac{1}{2\pi}$	$-\frac{1}{2} + .928067 i$	$\Gamma(1)$

The exact value of the critical exponent is $G(a_1, a_2, a_3; 1)$ and the asymptotic expansion follows from (4.3). Note that for all del Pezzo surfaces, $-\frac{\int J_3}{C^2} = (2\pi)^2$ in good agreement with the instanton numbers.¹⁹ If there is a star on $\int Jc_2$, we find an additional constant shift by one in the double-logarithmic solution (3.12). The monodromies are generated by the two shift operators at $x = 0$ and $x = 1$, which follow from the constants listed in the table.

There is an important difference between the $(\frac{1}{2}, \frac{1}{2}, 1)$ system and the other cases. It follows from the Riemann symbol that the former has a logarithmic solution at $\frac{1}{z} = 0$, while

¹⁹ This can be seen from the third Richardson transform. The asymptotic formula for the E_8 del Pezzo given in [30] is not quite correct. The monotonically increasing function n_d/n_d^{asym} would cross 1 at about $d = 100$.

the others have, as in the one-modulus compact three-folds [31], power series solutions at this point signaling a conformal field theory. In the compact case these can be identified as Gepner-type conformal field theories: tensor products of minimal $N = 2$ models.

The analytic continuation to $\frac{1}{z} = 0$ is particularly simple due to a Barnes integral representation – see [27][31][32] for similar applications. As in [32] it is easy to see that, given the above definition of t at $z = 0$, which corresponds to a choice of the B -field, one gets $t = \frac{1}{2}$ at $1/z = 0$, if $z = e^b x$ and $t = 0$ and at $1/z = 0$ if $z = -e^b x$. In particular, the \mathbf{P}^2 example has a conformal point at $1/z = 0$, which is the $\mathbf{C}^3/\mathbf{Z}_3$ non-compact orbifold.

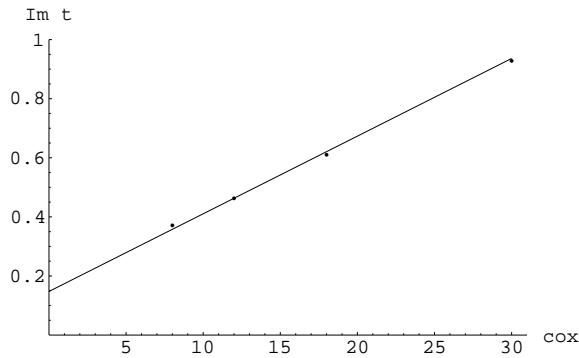


Fig. 5: Near linear dependence of the growth rate of instantons with the Euler (Coxeter) number.

Clearly it would be extremely interesting to find the physical system whose entropy of BPS states approaches in some limit the critical exponents which we have provided here. It is noteworthy that the coefficients $t_2(1)$ for the del Pezzo cases grow linearly (to a close approximation) with the Euler number assigned to the corresponding local Calabi-Yau, i.e. twice the Coxeter number of the associated group. If, as for K3, there is a bosonic string-like oscillator algebra on the moduli spaces, this would be the expected behavior. For example, in the local $\mathbf{P}^1 \times \mathbf{P}^1$ case, an oscillator-type partition function for some of the local invariants was found by Nekrasov and Kol [33], though the sense in which the coefficients were Euler characteristics of a moduli space remains unclear. This brings us to our next question.

4.2. What is the moduli space?

From the work of Gopakumar and Vafa II [1], we learn that the integers arising from a proper organization of the topological string partition functions simply encode the number

and properties of BPS states in the specified charge (homology class). Note that the BPS charges are specified by a homology class, not a genus. In fact, different genera are part of a connected moduli space of BPS states of specified charge.

The integers describe the representation content of the BPS states under an additional conjectural Lefschetz-type $SU(2)$ action on the cohomology of this moduli space. As is familiar from BPS counting on K3 [34][35], this moduli space is naively comprised of pairs of holomorphic curves together with flat $U(1)$ connections. This thinking may be too naive.

What is the proper definition of the moduli space? Experience is teaching us that D-branes can be thought of as objects in the bounded derived category of coherent sheaves. Indeed, this category is important for Kontsevich’s homological mirror conjecture [13]. The conjecture is that the derived category of coherent sheaves (D-branes/instantons in IIA/B) is equivalent to a category of Fukaya whose objects are Lagrangian (perhaps special-Lagrangian) objects (D-branes/instantons in IIB/A). This conjecture satisfies the correspondence principle. For example, it captures the idea of constructing the mirror Calabi-Yau through special-Lagrangian tori [36] as the equivalence of the moduli spaces of two distinguished objects (the structure sheaf of a point versus the distinguished toroidal Lagrangian submanifold). It also includes work of Vafa [37] by interpreting the three-point functions of massless excitations above a D-brane state as structure constants in the composition of morphisms – though Vafa has taken this further by identifying special coordinates through which to make identifications across mirror theories. Finally, ordinary mirror symmetry would be recovered by looking at similar considerations by treating the Calabi-Yau three-fold M as a (diagonal) D-brane in $M \times M$.

There is further evidence for the derived category. Hilbert schemes of points are a kind of intermediate step between moduli spaces of vector bundles and full-out derived moduli spaces, and they appear prominently in D-brane counts. Evidence also comes from requiring the Fourier-Mukai transform to act as a symmetry of objects for K3 compactifications [38]. As well, D-brane charges naturally live in K-theory [39][40]. For \mathbf{P}^2 these moduli spaces of objects are not well known, though some Poincaré polynomials of moduli spaces of points (sheaves supported on points or schemes of finite length) have been computed, as have some moduli spaces of higher-rank bundles. Heisenberg algebras have been found to act on cohomology, as for K3, which we take as loose evidence that these are the right spaces to study [41]. In addition, the exponential growth of the local invariants (with exponent depending on the “non-compact Euler number”) is in line with (super-)oscillator partition functions.

Let us now think of sheaves as one-term complexes, so as objects in a derived category. Then the moduli spaces of objects in this category should be the proper general framework for these questions. Moduli spaces of derived objects in general do not exist due to obstructions. For this reason, derived moduli spaces ²⁰ [42] may be the technology necessary to study the higher-genus integer invariants in the general case. Euler characters for such “spaces” can be defined. One can hope that this formulation of the question will lead to insight regarding the higher-genus problem for the quintic, which is not amenable to localization calculations.

Thinking of derived moduli spaces rather than moduli of sheaves is more in line with the spirit of Kontsevich’s mirror symmetry conjecture [13]. His motivation for introducing an A_∞ structure came in part from trying to define an extended moduli space of Calabi-Yau manifold as the moduli space of the structure sheaf of the diagonal M in $M \times M$ by deforming the associative algebra of functions as a homotopy associative differential graded (A_∞) algebra. The relation to the algebra to BRST cohomology classes on the conformal field theory of the D-brane, and of the grading to ghost number would be interesting to explore.

In fact, it is likely that we must treat our sheaves as sheaves in the total space of the canonical bundle of \mathbf{P}^2 . This would introduce further complexity.

4.3. Counting singular curves

For many applications, the differences between D-brane as cycle with bundle, as sheaf, or as derived object are unimportant. However, we may not be so lucky here. The argument in the second paper of [1] gives a heuristic derivation of $n_3^0(\mathbf{P}^2) = 27$. This should be equal to $\chi(\mathcal{M}_3)$, the Euler characteristic of the D-brane moduli space \mathcal{M}_3 of curves in the class $3H$, where H is the hyperplane class generating $H_2(\mathbf{P}^2)$. The n_d^g for $g \neq 0$ represent the different characters of the additional fiber-Lefschetz $SU(2)$ action on cohomology. $n_3^0(\mathbf{P}^2)$ is obtained by noting that the Jacobian of a smooth degree three curve can be identified with the curve itself (which has genus one). Therefore the choice of curve plus point on Jacobian is the same as the choice of curve plus point on curve. If we choose the point first (a \mathbf{P}^2 worth of such choices) and ask how many degree three curves pass through the point (a \mathbf{P}^8), we see \mathcal{M}_3 to be a \mathbf{P}^8 fibration over \mathbf{P}^2 , with Euler characteristic $9 \times 3 = 27$.

²⁰ “Derived quot schemes,” in fact, which retain all obstruction data in the form of a complex. In short, dg-schemes do not have tangent spaces, they have tangent complexes.

Following [35], one might attempt to count the Euler characteristic by noting that \mathcal{M}_3 must be a fibration over the moduli space of degree three curves in \mathbf{P}^2 , with fiber equal to the Jacobian of a given curve. As Jacobians of smooth curves have trivial Euler characteristic, we can localize our counting to the singular (more specifically, the rational curves). There is a moduli space of such curves (for K3 this space was zero dimensional), each of which should contribute some fixed amount determined by the singularity type. However, among the degree three curves we necessarily have reducible (e.g., $(X+Y)(X^2+Y^2+Z^2)=0 \subset \mathbf{P}^2$) and even unreduced (e.g., $(X+Y)^3=0 \subset \mathbf{P}^2$) curves. Here is where the sheaf interpretation is necessary. Over the unreduced curves, which can be thought of as multiply-wrapped branes, we should have rank k bundles (if k is the number of wrappings). These sheaves then have the same characteristic numbers as the non-singular curves. We are still unsure of how to perform the counting (e.g., there is a discrete infinity of higher-rank bundles over \mathbf{P}^1 with fixed degree). This interpretation is consistent with the moduli spaces of objects in the elliptic curve.

We can now hope to state Gopakumar and Vafa's approach as a conjecture that the Euler characteristics of the appropriate moduli dg-stack of derived objects on \mathbf{P}^2 of characteristic numbers ($r=0, c_1=d, c_2=d^2$) have Euler characteristic equal to n_d^0 . This conjecture might have to be tailored to account for the fact that the objects properly live on $K_{\mathbf{P}^2}$ with support in \mathbf{P}^2 . Whether we need the full weight of dg-stacks (which have tangent spaces which include all obstructions to deformations) to check this, remains to be seen. For the general situation, it is likely that we would.

These spaces may give some insight into the multiple cover formulas of Vafa and Gopakumar, as well. One also must find an additional fiber-Lefschetz $SU(2)$ action on the derived moduli spaces to agree with Vafa and Gopakumar's interpretation for $n_d^{g \geq 1}$. Exciting work lies ahead.

Acknowledgements

We are grateful to S. Katz, R. Pandharipande, T. Graber and C. Vafa for illuminating conversations. Also we would like to thank C. Faber for sending us his Maple program for the intersection calculation on $\overline{\mathcal{M}}_{g,n}$. The work of A. Klemm is supported in part by a DFG Heisenberg fellowship and NSF Math/Phys DMS-9627351.

References

- [1] C. Vafa and R. Gopakumar, “M-theory and Topological Strings-I & II,” hep-th/9809187, hep-th/9812127.
- [2] T.-M. Chiang, A. Klemm, S.-T. Yau, and E. Zaslow, “Nonlocal Mirror Symmetry: Calculations and Interpretations,” hep-th/9903053.
- [3] M. Bershadsky, S. Cecotti, H. Ooguri, and C. Vafa, “Holomorphic Anomalies in Topological Field Theories,” Nucl. Phys. **405B** (1993) 279-304.
- [4] M. Bershadsky, S. Cecotti, H. Ooguri, and C. Vafa, “Kodaira-Spencer Theory of Gravity and Exact Results for Quantum String Amplitudes,” Commun. Math. Phys. **165** (1994) 311-428.
- [5] W. Lerche, “Introduction to Seiberg-Witten Theory and its Stringy Origin,” Nucl. Phys. Proc. Suppl. **55B** (1997) 83-117, hep-th/9611190; A. Klemm, “On the Geometry behind N=2 Supersymmetric Effective Actions in Four-Dimensions”, Proceedings of the Trieste Summer School on High Energy Physics and Cosmology **96**, World Scientific, Singapore (1997) 120-242, hep-th/9705131; P. Mayr, “Geometric Construction of N=2 Gauge Theories,” Fortsch. Phys. **47** (1999) 39-63, hep-th/9807096.
- [6] S. Hosono, M.-H. Saito, and A. Takahashi, “Holomorphic Anomaly Equation and BPS State Counting of Rational Elliptic Surface,” hep-th/9901151.
- [7] M Marino and G. Moore, “Counting Higher Genus Curves in a Calabi-Yau Manifold,” Nucl. Phys. **B543** (1999) 592-614; hep-th/9808131.
- [8] M. Kontsevich, “Enumeration of Rational Curves via Torus Actions,” in *The Moduli Space of Curves*, Dijkgraaf et al eds., Progress in Mathematics **129**, Birkhäuser (Boston) 1995.
- [9] J. Li and G. Tian, “Virtual Moduli Cycles and Gromov-Witten Invariants of Algebraic Varieties,” J. Amer. Math. Soc. **11**, no. 1 (1998) 119-174.
- [10] K. Behrend and B. Fantechi, “The Intrinsic Normal Cone,” math.AG/9601010.
- [11] T. Graber and R. Pandharipande, “Localization of Virtual Classes,” math.AG/9708001.
- [12] C. Faber, “Algorithm for Computing Intersection Numbers on Moduli Spaces of Curves, with an Application to the Class of the Locus of the Jacobians,” math.AG/9706006.
- [13] M. Kontsevich, “Homological Algebra of Mirror Symmetry,” Proceedings of the 1994 International Congress of Mathematicians **I**, Birkhäuser, Zürich, 1995, p. 120; math.AG/9411018.
- [14] E. Witten, “Two-Dimensional Gravity and Intersection Theory on Moduli Space,” Surveys in Diff. Geom. **1** (1991) 243-310.
- [15] M. Kontsevich, “Intersection Theory on the Moduli Space of Curves and the Matrix Airy Function,” Commun. Math. Phys. **147** (1992) 1-23.

- [16] C. Faber and R. Pandharipande, “Hodge Integrals and Gromov-Witten Theory,” math.AG/9810173.
- [17] Brendan D. McKay, “*nauty* User’s Guide” available at <http://cs.anu.edu.au/~bdm/>.
- [18] E. Witten, “Phase Transitions in M-Theory and F-Theory,” Nucl. Phys. **471** (1996) 195-216; hep-th/96031150.
- [19] P. Aspinwall and D. Morrison, “Topological Field Theory and Rational Curves,” Commun. Math. Phys. **51** (1993) 245-262.
- [20] Yu. I. Manin, “Generating Functions in Algebraic Geometry and Sums over Trees” in “The moduli space of curves” (Texel Island, 1994), Progr. Math. **129**, Birkhäuser, Boston (1995) 401–417; alg-geom/9407005.
- [21] R. Pandharipande, “Hodge Integrals and Degenerate Contributions,” math.AG/9811140.
- [22] S. Katz, A. Klemm, and C. Vafa, “Geometric Engineering of Quantum Field Theories,” Nucl. Phys. **B497** (1997) 173-195.
- [23] S. Hosono, A. Klemm, S. Theisen and S.T. Yau, “Mirror Symmetry, Mirror Map and Applications to Calabi-Yau Hypersurfaces,” Commun. Math. Phys. **167** (1995) 301-350, hep-th/9308122; P. Candelas, A. Font, S. Katz and D. Morrison, “Mirror Symmetry for Two Parameter Models,” Nucl.Phys. **B429** (1994) 626-674, hep-th/9403187.
- [24] V. Batyrev, “Dual Polyhedra and Mirror Symmetry for Calabi-Yau Hypersurfaces in Toric Varieties,” J. Algebraic Geom. **3** (1994) 493-535.
- [25] The Bateman Project, *Higher Transcendental Functions*, Vol. 1, Sec. 5.3.-5.6, A. Erdelyi ed., McGraw-Hill Book Company, New York (1953).
- [26] D. Ghoshal and C. Vafa, “ $c=1$ String as the Topological Theory of the Conifold,” Nucl. Phys. **B453** (1995) 121.
- [27] P. Candelas, X. C. De La Ossa, P. Green, and L. Parkes, “A Pair of Calabi-Yau Manifolds as an Exactly Soluble Superconformal Theory,” Nucl. Phys. **B359** (1991) 21.
- [28] A. Klemm, P. Mayr, and C. Vafa, “BPS States of Exceptional Non-Critical Strings,” Nucl. Phys. **B** (Proc. Suppl.) **58** (1997) 177-194; hep-th/9607139.
- [29] W. Lerche, P. Mayr, and N. P. Warner, “Non-Critical Strings, Del Pezzo Singularities and Seiberg-Witten Curves,” hep-th/9612085.
- [30] J. A. Minahan, D. Nemechansky and N. P. Warner, “Partition function for the BPS States of the Non-Critical E_8 String,” Adv. Theor. Math.Phys. **1** (1998) 167-183; hep-th/9707149.
- [31] A. Klemm and S. Theisen, “Considerations of One-Modulus Calabi-Yau Compactifications: Picard-Fuchs Equations, Kähler Potentials and Mirror Maps,” Nucl. Phys. **B389** (1993) 153-180.
- [32] P. Aspinwall, B. Greene, and D. R. Morrison, “Measuring Small Distances in $N=2$ Sigma Models,” Nucl. Phys. **420** (1994) 184-242.

- [33] N. Nekrasov, “In the Woods of M-Theory,” hep-th/9810168.
- [34] M. Bershadsky, V. Sadov, and C. Vafa, “D-Branes and Topological Field Theories,” Nucl. Phys. **B463** (1996) 420-434; hep-th/9511222.
- [35] S.-T. Yau and E. Zaslow, “BPS States, String Duality, and Nodal Curves on K3,” Nucl. Phys. **B471** (1996) 503-512; hep-th/9512121.
- [36] A. Strominger, S.-T. Yau, and E. Zaslow, “Mirror Symmetry is T-Duality,” Nuclear Physics **B479** (1996) 243-259; hep-th/9606040.
- [37] C. Vafa, “Extending Mirror Conjecture to Calabi-Yau with Bundles,” hep-th/9804131.
- [38] P. S. Aspinwall and R. Y. Donagi, “The Heterotic String, the Tangent Bundle, and Derived Categories,” Adv. Theor. Math. Phys. **2** (1998) 1041-1074; hep-th/9806094.
- [39] R. Minasian and G. Moore, “K-Theory and Ramond-Ramond Charge,” hep-th/9710230.
- [40] E. Witten, “D-Branes and K-Theory,” hep-th/9810188.
- [41] See, e.g., H. Nakajima, “Lectures on Hilbert Schemes of Points on Surfaces,” preprint <http://kusm.kyoto-u.ac.jp/~nakajima/TeX.html>; I. Grojnowski, “Instantons and Affine Algebras I: The Hilbert Scheme and Vertex Operators,” Math. Res. Lett. **3**, no. 2 (1996) 275-291; and V. Baranovsky, “Moduli of Sheaves on Surfaces and Action of the Oscillator Algebra,” math.AG/9811092.
- [42] I. Ciocan-Fontanine and M. M. Kapranov, “Derived Quot Schemes,” math.AG/9905174.